



Simulation of Waves on Boom and Oil Plume Rising using Smoothed Particle Hydrodynamics

M. Rostami Hosseinkhani¹, P. Omidvar^{2†}, S. Allahyaribeik¹ and M. Torabi Azad³

¹Department of Marine Sciences, Graduate School of Natural Resources and Environment, Science and Research Branch, Islamic Azad University, Tehran, Iran

²Department of Mechanical Engineering, Yasouj University, Yasouj, Iran

³Department of Physical Oceanography, Faculty of Marine Science and Technology, Islamic Azad University, North Tehran Branch, Tehran, Iran

†Corresponding Author Email: omidvar@yu.ac.ir

(Received March 9, 2019; accepted May 22, 2019)

ABSTRACT

Marine oil spills can cause serious damage to the marine ecological environment. In the numerical modeling of oil plume rising and its advection, a better understanding of the oil plume transport may be effective on the sea pollution reduction and removing pollutants. In this paper, the effects of waves are investigated on the oil plume convection-diffusion pattern using smoothed particle hydrodynamics (SPH). Firstly, the rising patterns of an oil plume of different densities are simulated and the results are compared with the analytical solution. Then, the concentration distribution is shown for the oil plume rising problem. Afterwards, the suitability of the SPH method is examined by a cnoidal wave on shore effect. Finally, the plume of different conditions is located in waves and the advection of pollutant is studied with a fixed boom and different angles. It will be concluded that using a boom with a zero diversion angle would lead to minimum passing pollutant.

Keywords: Smoothed particle hydrodynamics; Two-phase currents; Oil plume rising; Concentration distribution.

NOMENCLATURE

C	concentration	u_g	plume rising velocity
c	sound speed	κ	interface curvature
d	water depth	d/dt	material derivative
Fr	Froude number	θ	boom angle
f	external forces	σ	surface tension coefficient
H	wave height	Π_{ij}	artificial viscosity
h	smoothing length	ϑ	kinematic viscosity
\hat{n}	unit vector perpendicular to the interface	δ_s	normalized function
P	pressure	ρ	density
R	plume radius		
T	wave period		
u	velocity		

1. INTRODUCTION

Oil pollution is one of the most predominant forms of sea pollution and it can cause a wide range of impacts in the marine environment. Dispersion of oil pollutants is one of the important problems in the marine environment and the increasing of oil pollution led different numerical models to be

developed. In the previous studies, (Hua & Lou, 2007) using the finite volume method and (Sultana, 2012) using the finite element, could predict the oil plume rising and dispersion pattern. The numerical modeling of a two phase current with complicated free surface in the vicinity of a boom is a challenging issue. Most of methods applied up to now are Eulerian's methods, while there are

Lagrangian methods used to examine two-phase flows.

The Smoothed Particle Hydrodynamics method is a mesh-free Lagrangian method to obtain numerical solutions of fluid governing equations. In this method, the fluid is considered as moving separate particles each of which has its own physical characteristics. A most important advantage of this method is solving free surface problems without any need to treat the free surface. Also, it has its own characteristics such as capability, coherence, and high accuracy to examine and analyze problems compared with other numerical methods. Moreover, for the problems involving more than one material where each material is described by its own set of particles, interface problems are found to be trivial in SPH in comparison with other methods e.g. finite difference schemes. In addition, the equations used in the SPH method are simpler in comparison with other methods and solid boundaries are implemented by a set of computational boundary particles that are interacting with fluid particles. However, the computational cost is one of the disadvantages of SPH because the time step is much smaller than the ones in other methods as explicit integration schemes are used.

The SPH method was introduced by (Gingold & Monaghan, 1977, Lucy, 1977) to examine astrophysics problems. Multi-phasic currents (Shao, 2012; Pourabdian *et al.*, 2017; Hu & Adams, 2006; Rostami & Omidvar, 2018), free surface currents (Violeau & Rogers, 2016, Omidvar *et al.*, 2015), Non-Newtonian fluids (Abdolahzadeh *et al.*, 2019; Omidvar & Nikeghbali, 2017; Shao & Lo, 2003), fluid and structure interactions (Omidvar *et al.*, 2012), heat transfer (Cleary & Monaghan, 1999b), and turbulent flows (Monaghan, 2011, Lo & Shao, 2002) are other applications of this method. SPHysics2D is an open source code to simulate free surface single phase problems. Here, this code is developed into two-phase fluids by adding the surface tension effect and an additional pressure term to the momentum equation for two fluids with density difference (such as water and oil). In the present study, and after Rostami and Omidvar (2018), the surface tension term provided by (Morris, 2000) was applied. In order to control the pressure between two phases, an additional pressure term provided by (Grenier *et al.*, 2009) was used. The rising pattern of a single plume with different densities is presented and the results are compared with available data. Simulating oil plume rise in a still water tank is aimed to validate and optimize the code of modeling different problems such as wave effect on oil plume convection and distribution. The convection-diffusion process and the concentration distribution are shown for the oil-plume rising problem. Then, the simulation of the cnoidal wave on beaches is conducted and compared with an available experimental result. Finally, the wave effect on oil plume convection and diffusion in the presence of a still boom on water was simulated. It will be shown that the SPH method is a useful tool for studying multiphase flows and convection-diffusion processes.

2. GOVERNING EQUATIONS

The fluid governing equations in a continuous medium as follows:

Mass conservation equation:

$$\frac{d\rho}{dt} = -\rho \nabla \cdot \mathbf{u} \quad (1)$$

And momentum conservation equation:

$$\frac{d\mathbf{u}}{dt} = -\frac{1}{\rho} \nabla P + \mathbf{f} \quad (2)$$

where d/dt , ρ , \mathbf{u} , p and \mathbf{f} are the material derivative, density, velocity, pressure, and gravity acceleration, respectively. The approach of the SPH method is to use particles carrying mass, density, pressure, viscosity, velocity, location, and other fluid characteristics. All terms of momentum and mass conservation equations could be discretized for two phases using this method by considering viscosity and surface tension. The particle different parameters are interpolated relative to neighbor particles to supply continuity.

In SPH methodology the continuous function $\phi(r)$ could be estimated for a particle located at distance r by the interpolation integral as below:

$$\phi(r) = \int_{\Omega} \phi(r') W(r-r', h) dr' \quad (3)$$

In the above equation, $W(r-r', h)$ is an interpolation function, in which h is the smoothing length. The above equation could be written as below by considering $m_j = \rho_j \Delta V_j$, where ΔV_j is domain volume of function $\phi(r)$:

$$\phi(r) = \sum_j \frac{m_j}{\rho_j} \phi(r_j) W(r-r_j, h) \quad (4)$$

where ρ_j and m_j are density and mass of the particle j , as well as $W_{ij} = W(r_i - r_j, h)$ is the interpolation function between particles i and j :

$$\phi(r_i) = \sum_j \frac{m_j}{\rho_j} \phi(r_j) W_{ij} \quad (5)$$

The $\phi(r_j)$ spatial derivative is:

$$\begin{aligned} \nabla \phi(r_j) &= -\sum_j \frac{m_j}{\rho_j} \phi(r_j) \nabla_j W_{ij} \\ &= \sum_j \frac{m_j}{\rho_j} \phi(r_j) \nabla_i W_{ij} \end{aligned} \quad (6)$$

In the SPH method, density is calculated based on two ways. Using the interpolation formula of the SPH method described in Eq. (5), density is calculated as below (Monaghan, 1992):

$$\rho_i = \sum_j m_j W_h(r_{ij}) \quad (7)$$

Based on the above equation, density of particles located near the surface is unreal due to their dependence on neighbor particles. Thus, the equation of density changes relative to time as (Monaghan, 2005):

$$\frac{d\rho_i}{dt} = \sum_j m_j \mathbf{u}_{ij} \cdot \nabla_i W_h(r_{ij}) \quad (8)$$

where \mathbf{u}_{ij} is velocity difference between particles i and j . As it is essential to calculate the interpolation function gradient in the continuity equation and also since the gradient of the interpolation function must be calculated in the conservation of momentum equation, therefore the second method is a better choice because the interpolation gradient can be calculated in a subroutine. For more information, readers are referred to (Grenier *et al.*, 2013).

Also, the momentum conservation equation could be discretized using the SPH method. The pressure gradient term is calculated as below:

$$\left(\frac{\nabla P}{\rho}\right)_i = \sum_j m_j \left(\frac{P_j}{\rho_j^2} + \frac{P_i}{\rho_i^2}\right) \nabla_i W_h(r_{ij}) \quad (9)$$

where P is the pressure. In order to simulate velocity of a two-phase flow, we have:

$$\frac{d\mathbf{u}_i}{dt} = -\sum_j m_j \left(\frac{P_i + P_j}{\rho_i \rho_j} + \Pi_{ij} + \right. \quad (10)$$

$$\left. R_{ij}\right) \nabla_i W_h(r_{ij}) + \mathbf{f}_s$$

In the above equation, R_{ij} and \mathbf{f}_s , and Π_{ij} are an added pressure, forces such as surface tension, and the viscosity term to consider the viscosity effects in the Euler equation, respectively.

The artificial viscosity is (Monaghan, 2005):

$$\Pi_{ij} = f(x) = \begin{cases} -\frac{\alpha hc}{\bar{\rho}_{ij}} \frac{\mathbf{u}_{ij} \cdot \mathbf{r}_{ij}}{r_{ij}^2 + \eta^2}, & \mathbf{u}_{ij} \cdot \mathbf{r}_{ij} < 0 \\ 0, & \mathbf{u}_{ij} \cdot \mathbf{r}_{ij} \geq 0 \end{cases} \quad (11)$$

where α is a constant between 0.01 and 1. Also, h , c , and $\bar{\rho}_{ij} = \frac{\rho_i + \rho_j}{2}$ are the smoothing length, sound speed, and average density, respectively. $\mathbf{u}_{ij} = \mathbf{u}_i - \mathbf{u}_j$ and $\mathbf{r}_{ij} = \mathbf{r}_i - \mathbf{r}_j$ are the velocity and the distance differences between particles i , and j , respectively. η is considered $0.1h_{ij}$ to prevent the denominator to become zero when two particles are getting closer to each other. The kinematic viscosity ϑ is proportional to $\frac{1}{8}\alpha hc$, and $\frac{\Delta u}{\Delta r}$ is similar to the spatial derivative of velocity. By disregarding η , the artificial viscosity for a two-phase flow is:

$$\Pi_{ij} = -\frac{16v_i v_j}{(v_i \rho_i + v_j \rho_j)} \frac{\mathbf{u}_{ij} \cdot \mathbf{r}_{ij}}{h |r_{ij}|} \quad (12)$$

The above equation is based on in which $\frac{\bar{v}_{ij}}{\bar{\rho}_{ij}}$ is replaced by $\frac{2v_i v_j}{v_i \rho_j + v_j \rho_i}$ as following:

$$\frac{\bar{v}_{ij}}{\bar{\rho}_{ij}} \rightarrow \frac{2v_i v_j}{v_i \rho_j + v_j \rho_i} \quad (13)$$

where R_{ij} is applied to control the pressure between two phases that its value is corrected by Monaghan and Rafiee as below (Monaghan & Rafiee, 2013):

$$R_{ij} = \mathcal{X} \cdot \left(\frac{\rho_{0,w} - \rho_{0,o}}{\rho_{0,w} + \rho_{0,o}}\right) \left|\frac{P_i + P_j}{P_i P_j}\right| \quad (14)$$

$\rho_{0,w}$ and $\rho_{0,o}$ are reference densities of water and plume, respectively. \mathcal{X} is a coefficient that is usually between 0.01 and 0.1 obtained based on numerical experiences and stability.

It is notable that surface tension plays an important role in problems such as the rising of oil plume in fluids like water. The fluid dynamic numerical method applied to calculate the surface tension should be extremely flexible for a better simulation of the interface of two immiscible fluids. The vertical surface tension is inserted on the interface of fluids is as (Morris, 2000, Hu & Adams, 2006):

$$F_s = f_s \cdot \delta_s \quad (15)$$

where δ_s is a normalized function and the force per unit area f_s is:

$$f_s = \sigma \kappa \hat{n} \quad (16)$$

where σ , \hat{n} , and κ are the surface tension coefficient, unit vector perpendicular to the interface, and interface curvature, respectively. It is assumed that surface tension of the whole fluid is constant and the surface gradient is negligible. f_s is inserted perpendicular to the interface and the local curvature. This force makes smooth areas of high curvature, reduce the total area, and decrease the surface energy.

We should choose δ_s to have a unit integral on the interface. In this condition, the physics of the interface is properly retrieved. Thus, δ_s could be (Morris, 2000):

$$\delta_s = |n| \quad (17)$$

where $|n|$ is the magnitude of the vector normal on the oil-water interface. The interface is routed by the color function,

$$c_i = \sum_j \frac{m_j}{\rho_j} c_j W_h(r_{ij}) \quad (18)$$

The color function equals to 1 for water particles and 2 for oil particles far from the oil-water interface, while it decreases to 0.4-0.5 near the free surface and the oil-water interface. The surface normal vector, unit normal vector, and the surface curvature are $n = \nabla c$, $\hat{n} = \frac{n}{|n|}$ and $\kappa = \nabla \cdot \hat{n}$, respectively. Based on above formulas, we have:

$$n_i = \sum_j \frac{m_j}{\rho_j} (c_j - c_i) \nabla W_h(r_{ij}) \quad (19)$$

$$\begin{aligned} \kappa &= (\nabla \cdot \hat{n})_i \\ &= \sum_j \frac{m_j}{\rho_j} (\hat{n}_j - \hat{n}_i) \cdot \nabla_i W_h(r_{ij}) \end{aligned} \quad (20)$$

The interface of a limit width is a surface with great variations of the color function. The interface width tends to zero when the number of particles tends to infinity. Out of the interface, n becomes small, while \hat{n} and κ become much greater which leads to calculate directions and values of surface tension improperly. In order to correct this error, \hat{n} could be filtered as below (Hu & Adams, 2006; Morris, 2000):

$$\begin{aligned} N_i &= \begin{cases} 1 & \text{if } |n_i| > \varepsilon \\ 0 & \text{otherwise} \end{cases} \\ \hat{n}_i &= \begin{cases} \frac{n_i}{|n_i|} & \text{if } |n_i| > \varepsilon \\ 0 & \text{otherwise} \end{cases} \end{aligned} \quad (21)$$

As $\varepsilon = \frac{0.01}{h}$, Eq. (20) becomes:

$$\begin{aligned} (\nabla \cdot \hat{n})_i^* &= \sum_j \min(N_i, N_j) \frac{m_j}{\rho_j} (\hat{n}_j \\ &- \hat{n}_i) \cdot \nabla_i W_h(r_{ij}) \end{aligned} \quad (22)$$

Also, more accurate solutions could be obtained by normalizing the curvature line as

$$\begin{aligned} \kappa &= (\nabla \cdot \hat{n})_i \\ &= \frac{\sum_j \min(N_i, N_j) \frac{m_j}{\rho_j} (\hat{n}_j - \hat{n}_i) \cdot \nabla W_h(r_{ij})}{\sum_j \min(N_i, N_j) \frac{m_j}{\rho_j} W_h(r_{ij})} \end{aligned} \quad (23)$$

The surface tension acceleration a_s is:

$$(a_s)_i = -\frac{\sigma_j}{\rho_j} (\nabla \cdot \hat{n})_i n_i \quad (24)$$

Considering the momentum equation changes for two-phase flows and surface tension effects, we could rewrite the momentum equation as below:

$$\begin{aligned} \frac{du_i}{dt} &= -\sum_b m_j \left(\frac{P_i + P_j}{\rho_i \rho_j} + \Pi_{ij} + R_{ij} \right) \nabla_i W_h(r_{ij}) \\ &+ (a_s)_i \end{aligned} \quad (25)$$

The diffusion phenomenon is described by the Fick's law of diffusion based on which there is a proportion between the mass flow diffusion and concentration gradient (Fick, 1855). By neglecting convection phenomenon, the diffusion equation is:

$$\frac{dC}{dt} = D \nabla^2 C \quad (26)$$

in which C and D are concentration and diffusion coefficients, respectively. If the current is two-phasic with little density difference (for example water and oil), convection does not significantly affect the diffusion phenomenon. The convection-diffusion equation is (Fischer *et al.*, 1979):

$$\frac{dC}{dt} = D \nabla^2 C - \nabla \cdot (vC) \quad (27)$$

Also, the convection-diffusion equation in the SPH form is:

$$\begin{aligned} \frac{dC_i}{dt} &= \sum_{j=1}^N \frac{m_j}{\rho_i \rho_j} \frac{4D_i D_j}{D_i + D_j} (\rho_i + \rho_j) \frac{r_{ij} \cdot W_{ij}}{r_{ij}^2 + \eta^2} C_{ij} \\ &- \sum_{j=1}^N m_j \frac{C_i}{\rho_i} v_{ij} \cdot \nabla_i W_{ij} \end{aligned} \quad (28)$$

in which $\eta^2 = 0.01h$ in order to prevent the denominator to become zero when two particles are very close.

Water is usually considered as an incompressible fluid. Thus, pressure is calculated by the Poisson's equation. As there is not separate any pressure equation for incompressible fluids like water, an artificial state equation is used in which the sound velocity should meet the compressibility condition. Based on, (Monaghan, 1994) and (Batchelor, 2000) defining a relation between pressure and density, we use the following state equation:

$$p = B \left[\left(\frac{\rho}{\rho_0} \right)^\gamma - 1 \right] \quad (29)$$

In this equation, pressure is calculated in terms of Pascal, reference pressure is $B = \frac{\rho_0 c_0^2}{\gamma}$, γ is a constant which is considered 7 for a fluid consisting of water and a fluid (800 kg/m³) like oil (Grenier *et al.*, 2013). ρ_0 is the reference density which is 1000 kg/m³ for water. B is a constant, and the sound velocity (c_0) should be ten times of the maximum velocity of fluid particles.

As mentioned above, the interpolation function is of great importance in the SPH method as quantities are calculated by using this function. It determines the area affected by each particle. Based on (Morris *et al.*, 1997) the interpolation function is:

$$W(r_{ij}) = \frac{1}{h^q} f\left(\frac{r_{ij}}{h}\right) \quad (30)$$

where ϑ is the system dimension, and $h = 0.92\sqrt{\Delta x^2 + \Delta z^2}$ with Δx and Δz being the initial horizontal and vertical distance between particles.

There are different kinds of interpolation functions in the SPH method. As shown below, the Wendland interpolation function is used in this study (Wendland, 1995):

$$W(|r-r'|, h) = \frac{k}{h^q} \times \begin{cases} (1+2q)(2-q)^4 & 0 \leq q < 2 \\ 0 & q \geq 2 \end{cases} \quad (31)$$

where k is normalization constant with the values of $\frac{3}{4}$, $\frac{7}{4\pi}$ and $\frac{7}{8\pi}$ in one, two, and three dimensions calculations, respectively.

Boundary condition is one of the most important aspects of each numerical simulation. The SPH method has different boundary conditions to simulate boundaries such as dynamic Dalrymple dynamic boundary conditions and Monaghan repulsive force (Dalrymple *et al.*, 2002, Monaghan & Kos, 1999), which is one of the SPH method weaknesses.

In this study, the repulsive force method provided by Monaghan was applied for boundary conditions (Monaghan, 1989). Based on the free surface boundary condition, the surface pressure is zero. The SPH method has different time algorithms of which the predictive-corrective is used in this study (Monaghan, 1989).

In order to validate the developed code, problems such as an oil plume rise with the density ratio $\rho_1/\rho_2 = 40$ and 1.25 in a still water tank, distribution of oil plume concentration in a still water tank, and a one-phase wave in shore were validated.

3. RESULTS

In order to validate the developed code for a two-phase current, the problem of an oil plume rising (of $\rho_1/\rho_2 = 40$ and $\mu_1/\mu_2 = 85$) in a still water tank is examined here. Results of the numerical model are used as reference data (Sultana, 2012). Initial conditions can be seen in Fig. 1 in which the plume radius is 0.25 m.

As seen in Fig. 2, the SPH method results for oil plume rise are compared with results of Sultana numerical solution at different times (Sultana, 2012).

As seen in Fig. 2, there is a good agreement between results of the developed SPH model and the finite element model.

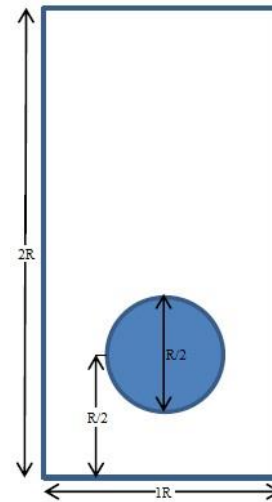


Fig. 1. The initial geometry of oil plume rise ($\rho_1/\rho_2 = 40$).

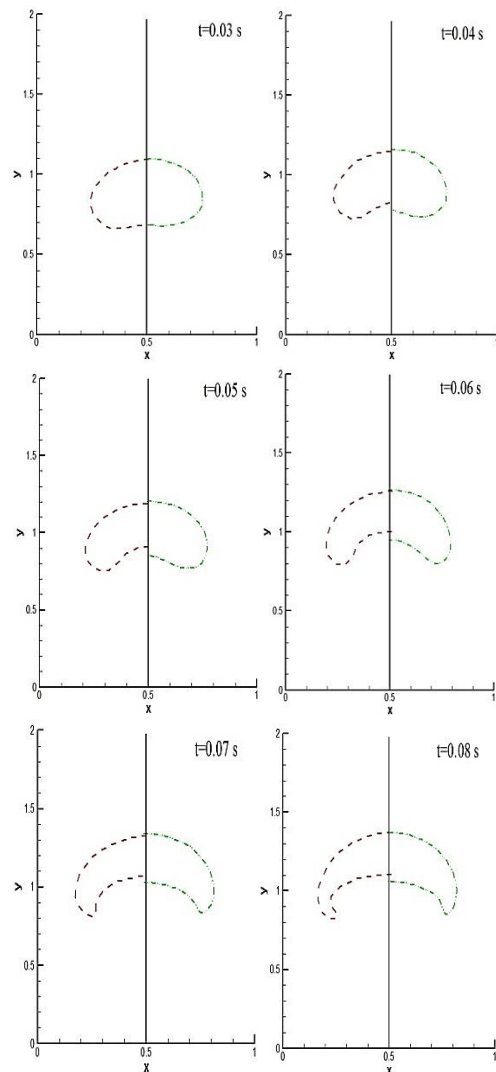


Fig. 2. Oil plume rise ($\rho_1/\rho_2 = 40$): the Sultana numerical solution is at the left of each panel and the SPH method solution is at the right side.

In order to validate the results for a two-phase current with density difference of $\rho_1/\rho_2 = 1.25$, the problem of oil plume rising in water was examined. Based on initial conditions shown in Fig. 3, $R = 1$.

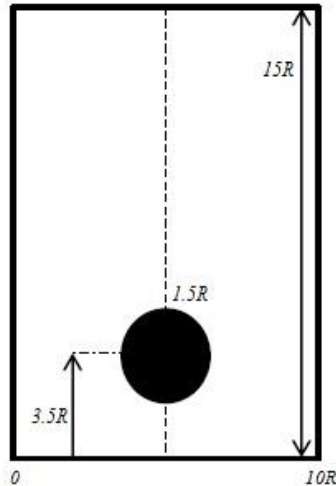


Fig. 3. Initial geometry of oil plume rise in a still water tank ($\rho_1/\rho_2 = 1.25$).

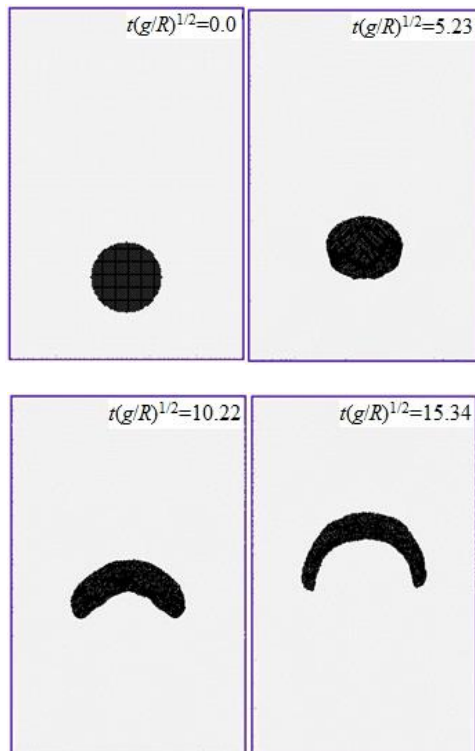


Fig. 4. Oil plume rise in a still water tank at different times.

As the water tank is still, there is a good symmetry in the Fig. 4 which continues over time. For water and oil, $\gamma = 7$ and the surface tension coefficient is considered to be 0.032. In order to validate the oil

plume rise, the below formula for analytical solution is used (Batchelor, 2000):

$$Z(t) = Z_s + \frac{1}{2} \sqrt{\frac{\rho_w - \rho_o}{\rho_w} g R} t \quad (32)$$

in which $Z(t)$ is the distance at each time, Z_s is the initial distance, t is time, ρ_o and ρ_w are the density of oil and water, respectively, and R is the plume radius.

The highest point of the oil plume is calculated at each time and compared with the analytical solution.

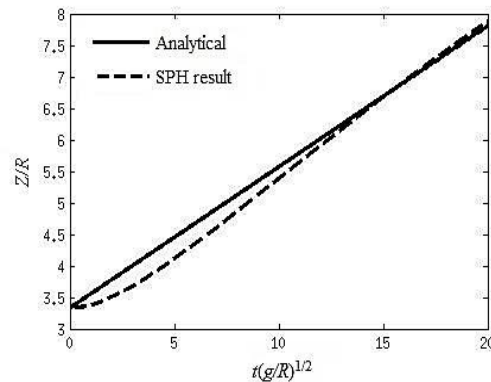


Fig. 5. A comparison between numerical and analytical solution of the oil plume rise in a still water tank in terms of dimensionless time.

Comparing the analytical solution with results of the SPH method, we calculated the mean absolute error as shown below (Omidvar *et al.*, 2012):

$$MAE = \frac{1}{n} \sum_{i=1}^n |Z_i^* - Z_i| \quad (33)$$

MAE is the mean absolute error, Z_i^* is the location at each time step, and n is the number of particles. Based on the diagram of the oil plume rise in a still water tank, $MAE = 0.1434$. As seen in Fig. 5, there is a good agreement between analytical solution and SPH results according to the mean error.

3.1 The Distribution of Rising Oil Plume Concentration in the Still Water Tank

In this problem, the convection and diffusion of a 2-D two-phasic current (oil and water) is examined by the SPH method ($\rho_1/\rho_2 = 1.25$). The initial condition is a tank by length and width of 2.4m at the center of which there is an oil plume of 0.2m radius. The problem initial conditions are shown in Fig. 6.

Based on the geometry of oil plume rise, the distribution of oil plume concentration at the initial moment is assumed as below (Aristodemo *et al.*, 2010):

$$C(x, z, t = 0) = \exp \left[-\frac{(x - x_0)^2}{4D} - \frac{(z - z_0)^2}{4D} \right] \quad (34)$$

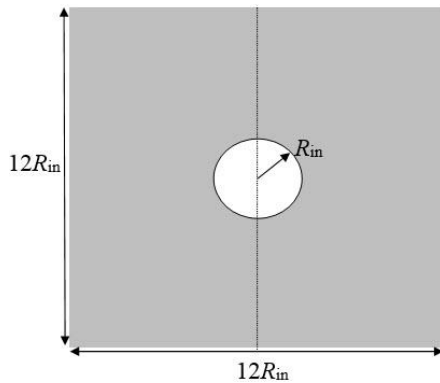


Fig. 6. The initial geometry of oil plume.

The plume center is located at (x_0, y_0) , and D is the diffusion coefficient. The analytical solution is:

$$C(x, z, t) = \frac{c_0}{\sqrt{t + t_0}} \exp \left[-\frac{(x - x_0)^2}{4D(t + t_0)} - \frac{(z - z_0 - Vt)^2}{4D(t + t_0)} \right] \quad (35)$$

In this equation, $t_0 = 1$ s, $c_0 = 1$ kg.s^{1/2}/m³, and V is the mean velocity of oil plume rise.

$$V = \frac{1}{2} \sqrt{g \frac{\rho_w - \rho_o}{\rho_w} r} \quad (36)$$

The distribution of oil plume in a still water tank at different times is shown in Figs. 7 and 8. The distribution of oil plume concentration for two diffusion coefficients, 10^{-3} and 10^{-4} , is compared with the analytical solution at different times which shows a good fit between the analytical solution and the distribution of oil plume concentration.

As seen in Figs. 7 and 8, there is a good agreement between the analytical solution and the distribution of oil plume concentration using the SPH method. Also, the oil plume rise and its diffusion velocity decreased during 0.5s due to the plume deformation. Moreover, the oil plume concentration is reduced as the diffusion velocity is decreased. Based on results, the distribution of concentration may be examined by the SPH method. This simulation is applied to predict the concentration pattern of two-phase currents.

3.2 Validation of Cnoidal Wave on Shore

A cnoidal wave on shore was simulated in this problem. A water tank of 24 m length has 1:35

gradient at the right side. Water depth (d), wave height (H), and wave period (T) were 0.4 m and 0.12 m, and 2 s respectively. The problem initial geometry is shown in Fig. 9.

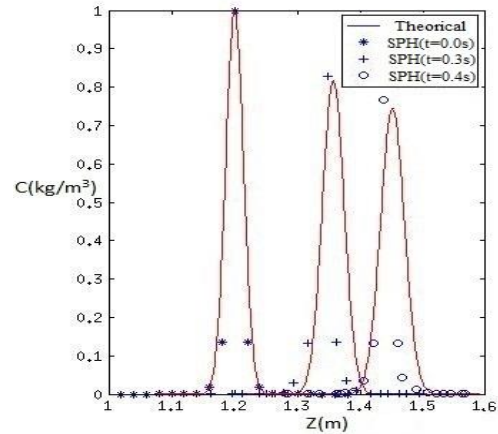


Fig. 7. A comparison between the distribution of oil plume concentration in analytical and SPH method solutions at different times for $D = 10^{-4}$ m²/s.

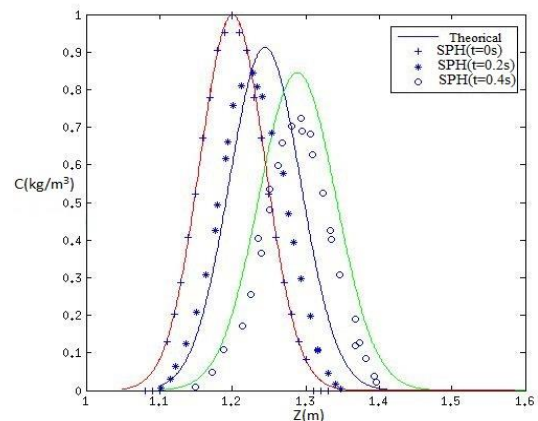


Fig. 8. A comparison between the distribution of oil plume concentration in analytical and SPH method solutions at different times for $D = 10^{-3}$ m²/s.

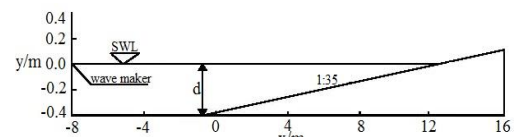


Fig. 9. Initial geometry of water tank of cnoidal wave on shore.

To validate the wave on shore, six points on the gradient were chosen and the free surface height at different locations were compared with results of (Zheng *et al.*, 2009) measurements which can be seen in the Fig. 10.

To validate the wave, the problem of a cnoidal wave on shore were simulated which it is found that

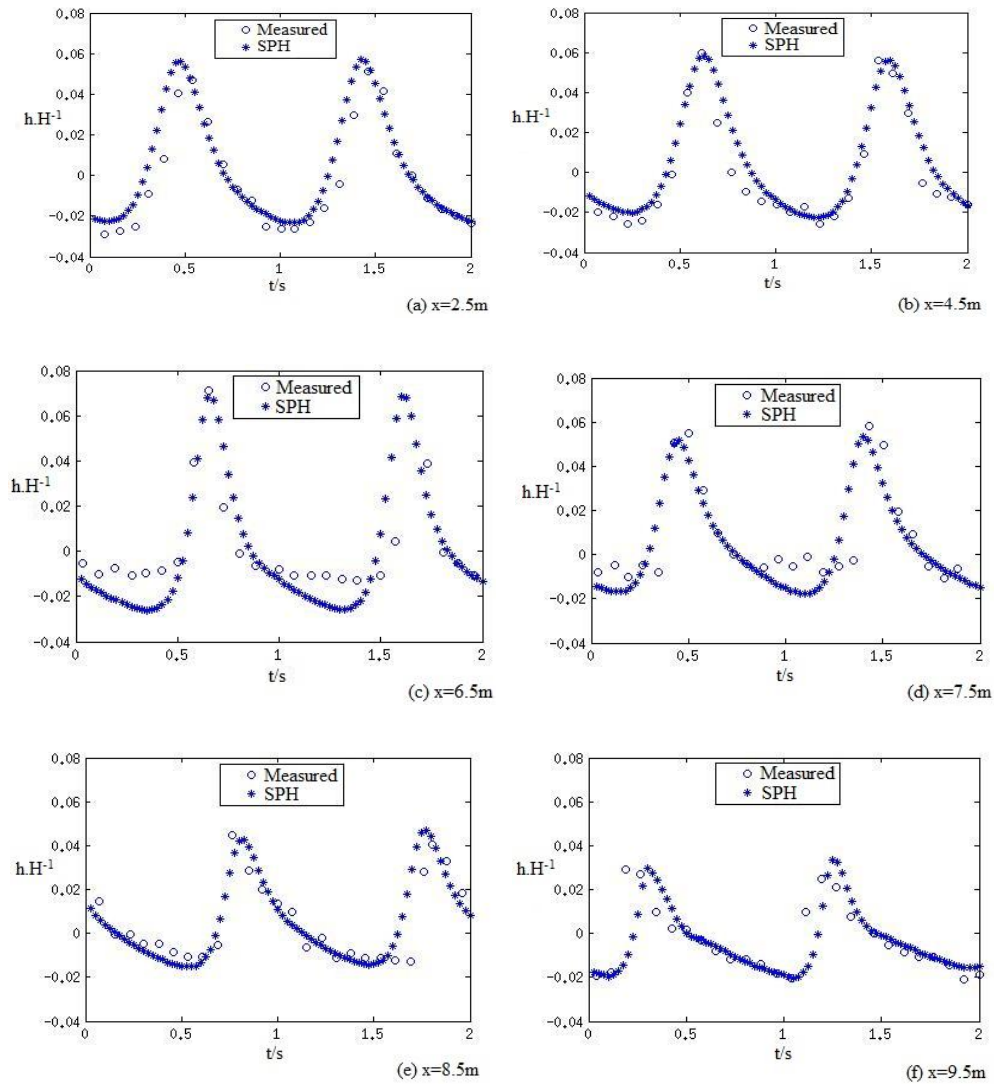


Fig. 10. Free surface height at different locations.

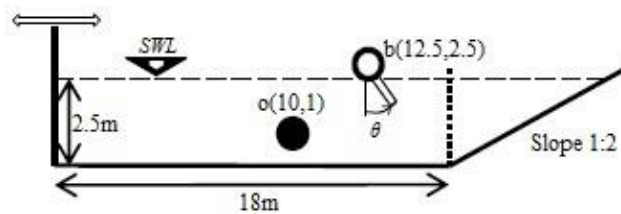


Fig. 11. Initial geometry of cnoidal wave on a sloped shore in which there is a motionless boom.

the SPH method has acceptable results compared with measurement results. Based on validated results, the SPH method is a proper way to examine the behavior of oil plume in water and its concentration distribution. Thus, this method is applied to simulate some problems in different conditions to examine the distribution of plume concentration.

3.3 The Wave Effect on Oil Plume Rise

A plume is a column of one fluid moving through

another. Several effects control the motion of the fluid, including momentum (inertia), diffusion and buoyancy (density differences). In this problem, the wave effect on oil plume convection and diffusion in the presence of motionless boom on water was simulated. The water tank was of length 25 m and gradient 1:2. Water depth d was 2.5 m, wave height H was 0.3 m, and wave period T was 2 s. Also, the piston height was 4 m. The problem initial geometry is shown in Fig. 11.

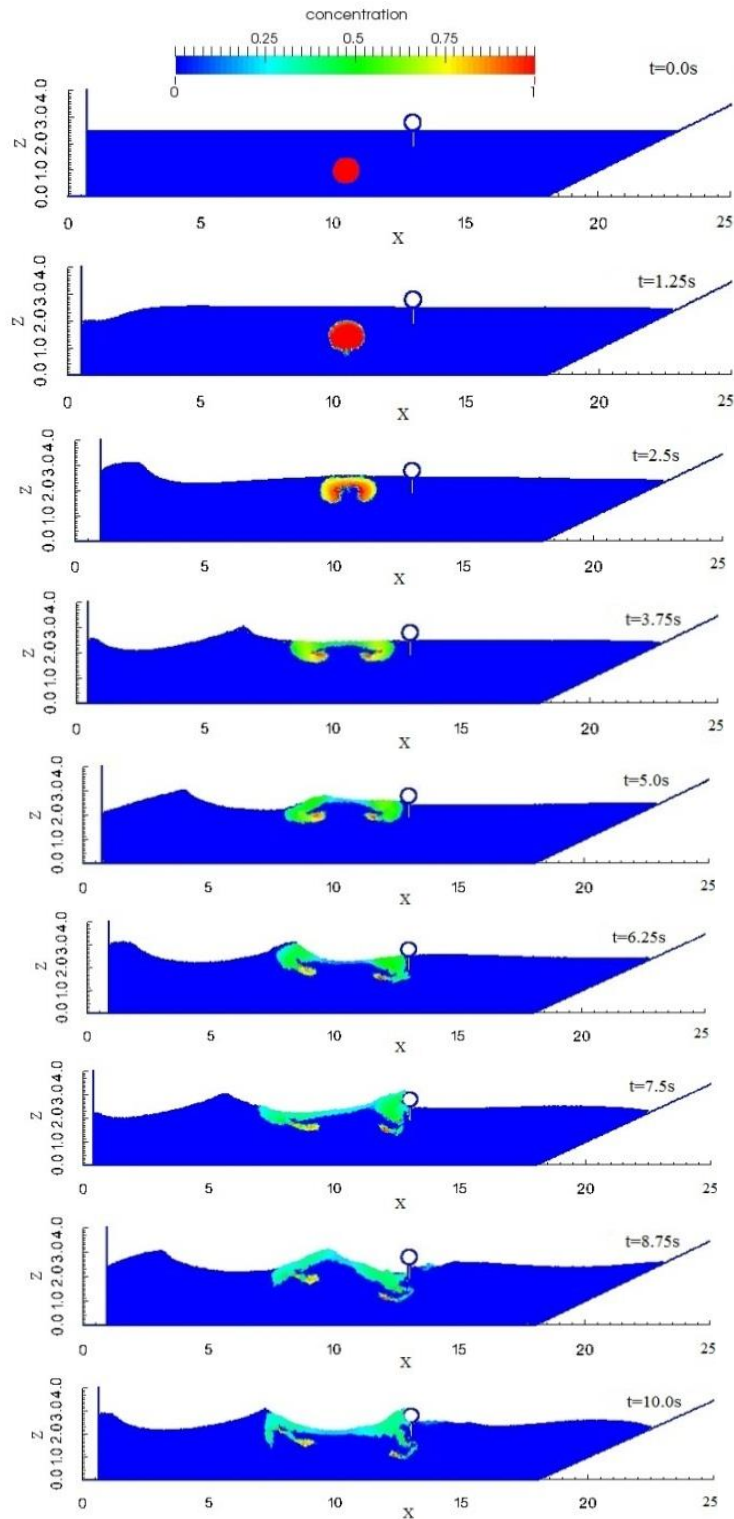


Fig. 12. Wave effect on oil plume convection and diffusion on a shore in which there is a motionless boom.

Based on results, the SPH method is a great way to examine the wave effect on the oil plume convection and diffusion in water. As seen in Fig. 12, oil plume around the boom, which prevents from oil plume convection and diffusion, had risen

symmetrically for 3.75 s before wave reached there. After, it rose asymmetrically. As seen in Fig. 13(a), just a part of oil plume of less concentration tend to pass under the boom and other parts of more concentration cannot pass from boom over time.

According to Fig. 13(b), a part of oil plume of less concentration passed the boom at $t = 10$ s, and other parts of more concentration (in red) remained behind the boom.

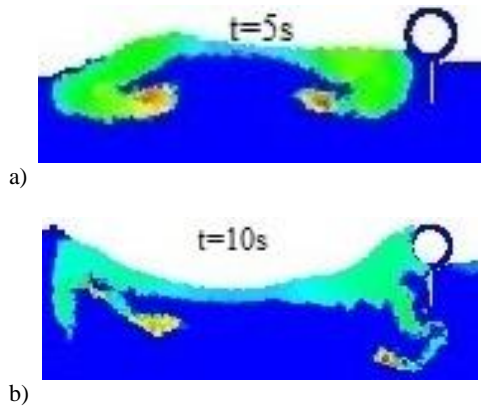


Fig. 13. Oil plume concentration at 5s and 10s.

The distribution of oil plume concentration at different times is shown in Fig. 14. As shown in the figure, the distribution of oil plume concentration decreases in time.

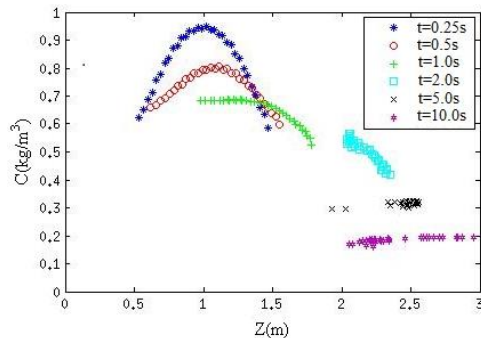


Fig. 14. A comparison between the distribution of oil plume concentration at different times.

3.4 Boom Effects with Different Angles on the Oil Plume Dispersion

In this problem, the effects of a boom with different angles on the oil plume dispersion are investigated. As seen in Fig. 15, the percentage of oil plume passed was compared for three different angles and it was found that the least percentage of oil passed the boom at an angle of 0° . Table 1 shows the effect of boom angle variation on the passing plume percentage after 10 seconds. It should be mentioned that the passing plume percentage is 55% when there is no boom at $t = 10$ s.

3.5 The Wave Height Effect on Oil Plume Dispersion

In this section, the wave height effect on oil plume dispersion with boom angle 0° has been simulated.

According to Fig. 16, it can be seen that an increase in the wave height led to more percentage of oil plume passed the boom. Table 2 shows the effect of wave height on the passing plume percentage after 10 seconds.

Table 1 Effect of boom angle variation on the passing plume percentage in 10 seconds

passing plume percentage at $t = 10$ s	Boom angle
1.15%	$\theta=0^\circ$
2.30%	$\theta=-30^\circ$
2.53%	$\theta=+30^\circ$

Table 2 Effect of wave height on the passing plume percentage in 10 seconds

passing plume percentage	H/d
0%	0.04
0%	0.08
1.38%	0.12
2.07%	0.16
4.37%	0.20

3.6 The Plume Radius Effects on Oil its Dispersion

In the following, convection and diffusion of oil plume on shore affected by different plume radii were simulated. The percentage of oil plume passed for different radii are shown in Fig. 17 from which it can be seen that an increase in the radius led to more percentage of oil plumes passed the boom. Table 3 shows the effect of plume radius on the passing plume percentage after 10 seconds.

Table 3 Effect of plume radius on the passing plume percentage in 10 seconds for different boom angle

R/d	$\theta=-30^\circ$	$\theta=0^\circ$	$\theta=+30^\circ$
0.1	0%	0%	0%
0.2	2.30%	1.38%	2.53%
0.3	8.04%	6.31%	9.47%
0.4	13.77%	10.73%	15.55%

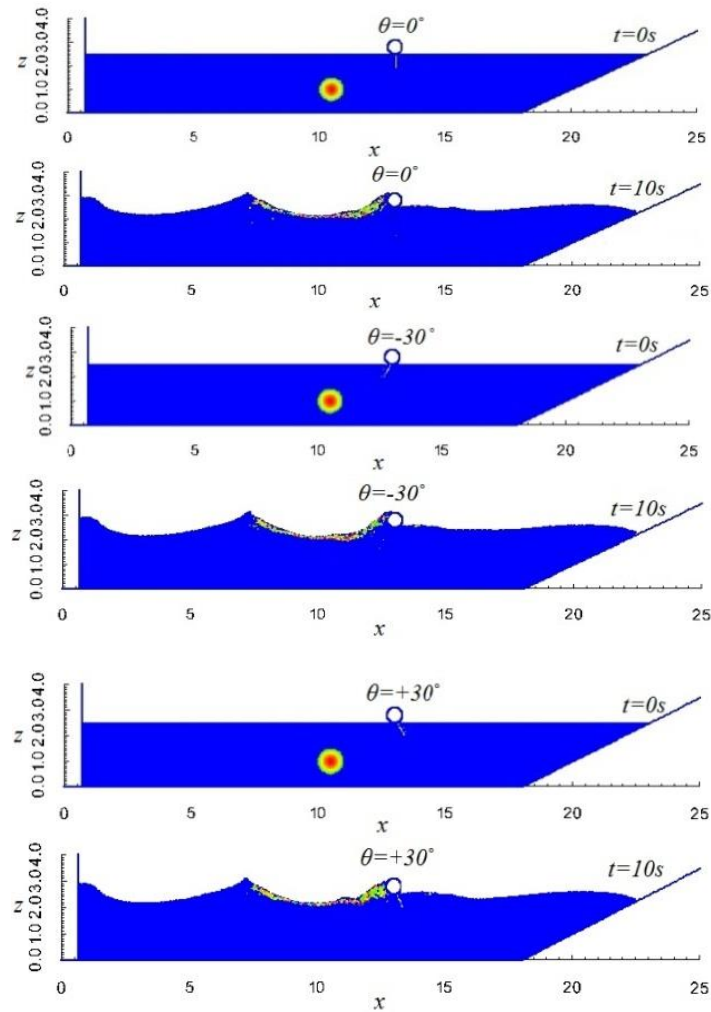


Fig. 15. Simulation of the effect of boom with different angle on the oil plume dispersion after 10 seconds.

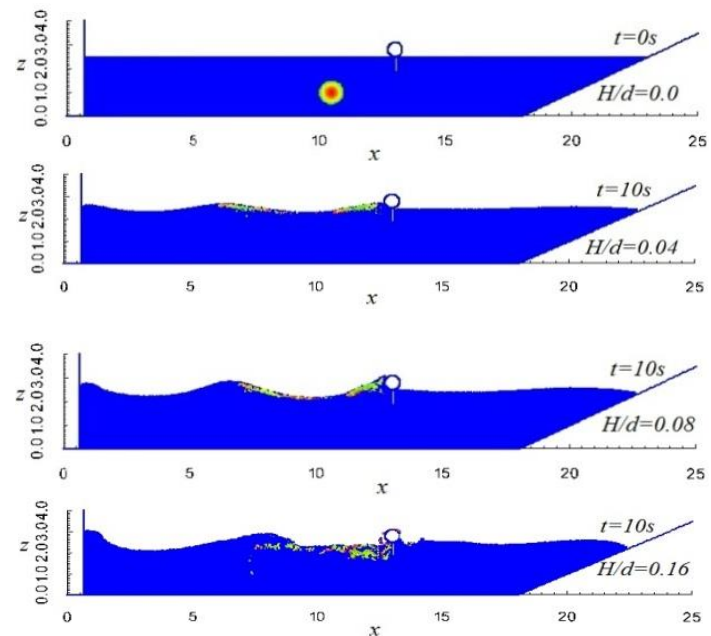


Fig. 16. Simulation of the effect of wave height with boom angle 0° on the oil plume dispersion after 10 seconds.

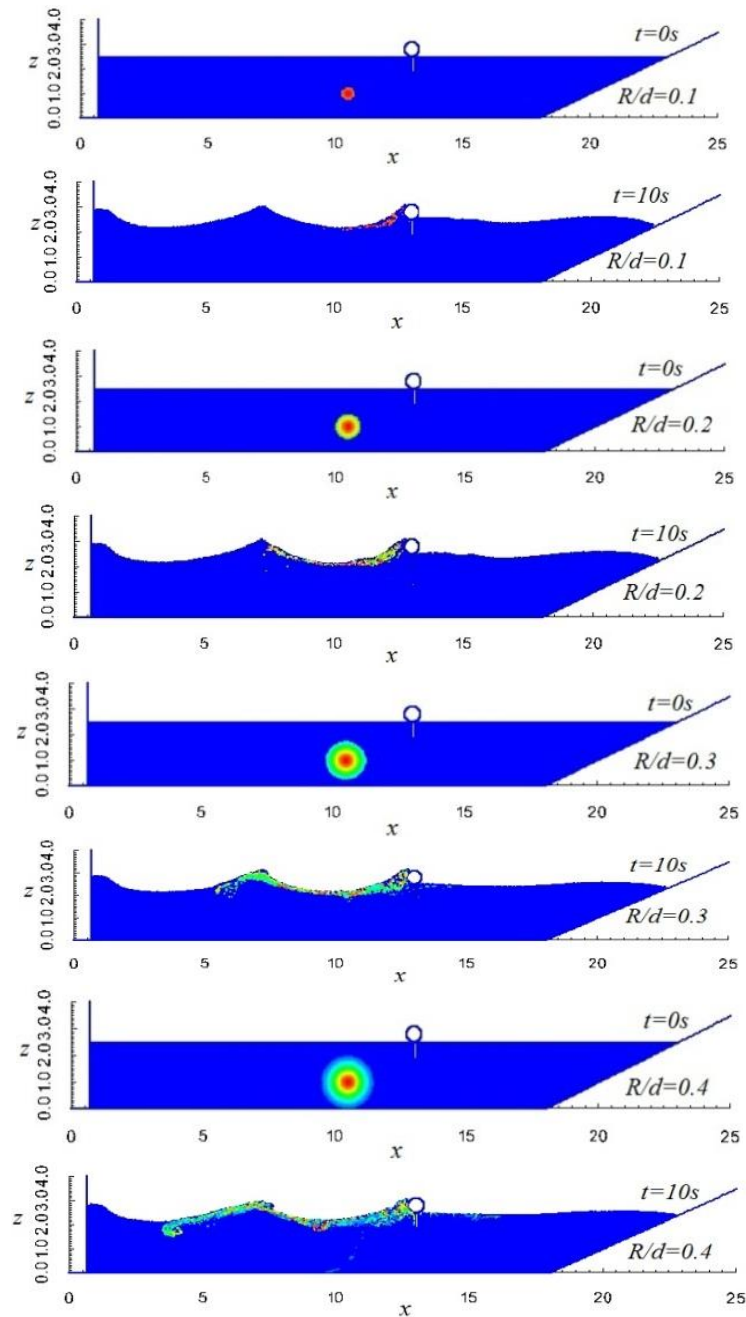


Fig. 17. Simulation of the effect of plume radius with boom angle 0° on the oil plume dispersion after 10 seconds.

Figure 18 shows comparison of the effect of oil plume radius with different boom angle on the passing plume percentage and Fig. 19 shows comparison of the effect of different wave height on the passing plume percentage after 10 seconds.

3.7 The Froude Number Effect on Oil Plume Dispersion

Based on the results, the SPH method for two-phase currents with density difference is suitable to examine the behavior of oil plume in a shore to

show concentration distribution in different conditions.

As a result, this method is applied to simulate and examine the distribution of oil plume concentration under different conditions. It is notable that no heat transfer was considered. Here, the effects of plume rising velocity on its convection and diffusion in the presence of a still boom are examined. This problem was aimed to examine the effects of plume rising velocity on its distribution.

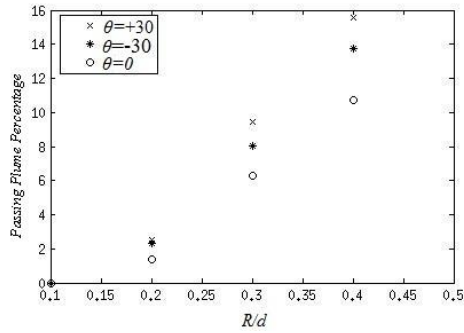


Fig. 18. Effect of plume radius with different boom angles versus the passing plume percentage at $t=10s$.

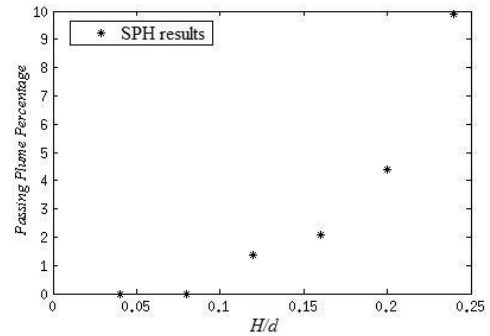


Fig. 19. Effect of different wave heights versus the passing plume percentage at $t=10s$.

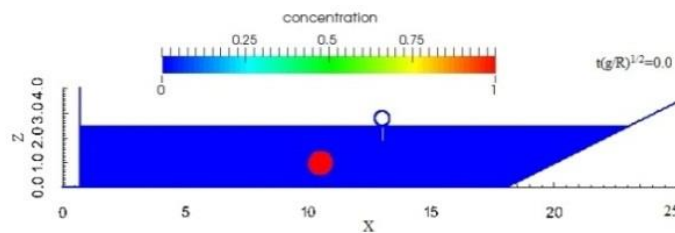


Fig. 20. Concentration distribution of oil and water at $t(g/R)^{1/2}=0.0$.

3.8 The Concentration Distributions of Oil Plume in a Shore with Different Froude Numbers

In this problem, the concentration distribution of oil plume of radius $0.5R$ in a sloped shore was examined. Diffusion coefficient is defined $10^{-1} \text{ m}^2/\text{s}$ and the problem initial geometry is shown in Fig. 11.

As seen in Fig. 20, the concentrations of oil and water plumes were considered 0 and 1, respectively.

$$C_{avg}^* = \frac{C}{C_{max}} \quad \tau = t \sqrt{\frac{g}{R}}$$

In this section, time and concentration were made dimensionless. C_{avg}^* is the average concentration of all particles. Afterward, concentration means dimensionless concentration which was made dimensionless by the average and maximum concentrations. The concentration distribution of rising plume at different dimensionless times is shown in Fig. 21. Here, the Froude number is calculated based on $Fr = \frac{u_g}{\sqrt{gL}}$ where u_g is the plume rising velocity and g is the gravity accelerations. In this case $L = 2R$ and R is the initial radius of the plume.

In this problem, the effect of plume rising velocity on its convection and diffusion in the presence of a still boom was considered. As seen in Fig. 21, concentration distribution of rising oil plumes with Froude numbers of 0, 1, 2 and 3 for dimensionless time $t(g/R)^{1/2}$ equal to 31.32, was simulated.

According to Fig. 21, it can be seen that an increase in the Froude number led to higher percentage of oil plume passing the boom. Also, oil plume was more diffusion in water and oil concentration was more reduced.

Comparing different Froude numbers was aimed to examine the effect of plume rising velocity on the concentration distribution at different times. The average concentration of oil and water plumes at different times are shown in Figs. 22 and 23, respectively, in which the average concentrations of oil plume with different Froude number are compared.

As seen in Figs. 22 and 23, there is a concentration transport from oil plume of the maximum concentration to water of the minimum concentration. Thus, the plume concentration decreases while water concentration increases.

It is notable that concentration transfers from the region of more to less concentration. As seen in Fig. 22, oil plume diffusion in water is more for a larger Froude number because the plume rising velocity is more. The reason of an increase in diffusion is that plumes do not mix and occupy more space of water due to higher velocity of the plume. As a result, the contact surface of plume with water was increased, oil was more diffused in water, and oil concentration was more reduced. According to what is seen in Fig. 23, large Froude numbers lead to more water concentration. As shown in Fig. 24, the mean concentration decreases as the Froude number increases.

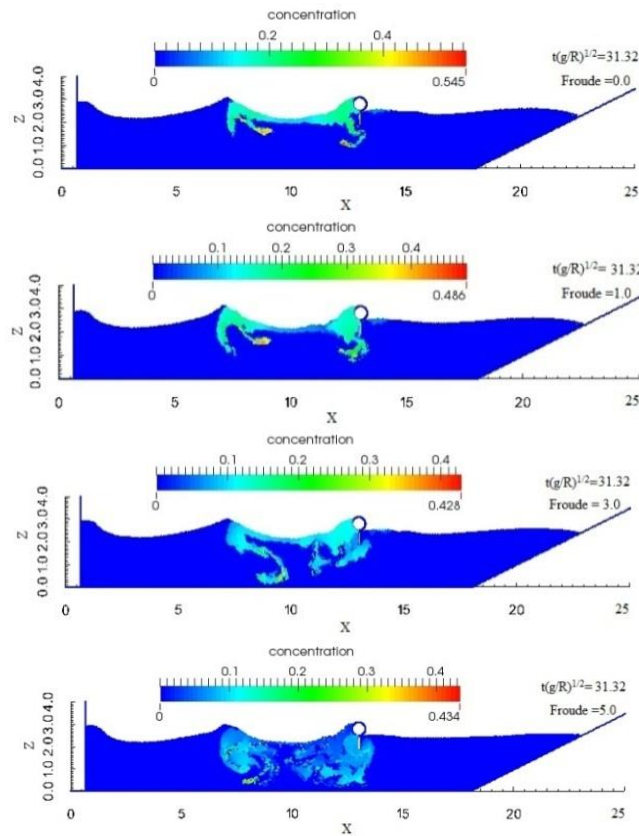


Fig. 21. Concentration distributions of oil plume in a shore with different Froude numbers.

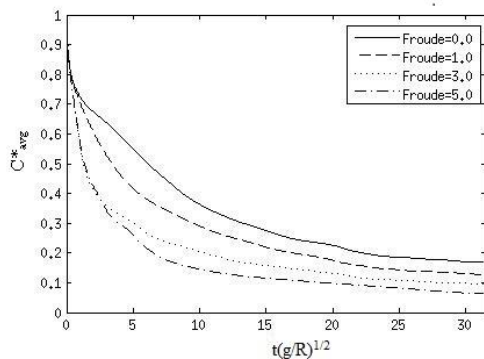


Fig. 22. A comparison between oil average concentration of oil plume with different Froude numbers at different times.

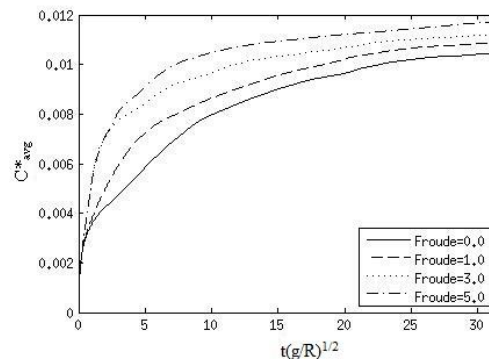


Fig. 23. A comparison between water average concentration of oil plume with different Froude numbers at different times.

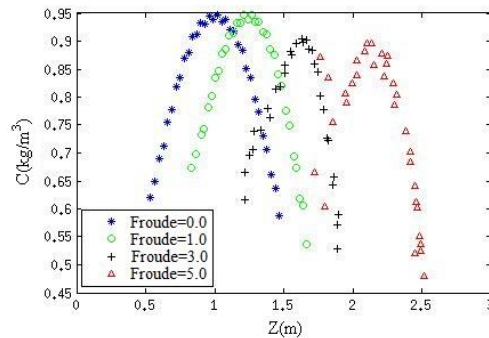


Fig. 24. A comparison between the distribution of oil plume concentration with different Froude number at $t(g/R)^{1/2}=0.8$.

4. CONCLUSION

In this work, the wave effects on the oil plume convection and diffusion process were simulated, where the SPHysics2D code was developed for two-phase flows by taking the surface tension effects into account. First and in order to validate the two-phase code, a single oil plume rising were investigated in a still water tank by looking carefully at its convection-diffusion effects. Then, the simulation of the cnoidal and single-phase waves on a beach is conducted and results were successfully compared with an available experimental data. As seen in results, oil plume diffusion in water is more for a larger Froude number due to a larger velocity. It was concluded that the SPH method is proper to study two-phase currents and the mechanism of convection-diffusion due to its unique features to examine the wave effects on the oil plume concentration distribution.

REFERENCES

- Abdolahzadeh, M. A. Tayebi and P. Omidvar (2019). Mixing Process of two-phase non-Newtonian fluids in 2D using Smoothed Particle Hydrodynamics. *Computers & Mathematics with Applications*.
- Aristodemo, P., I. Federico and P. Veltri (2010). Two-phase SPH modelling of advective diffusion processes. *Environmental Fluid Mechanics* 10(4), 451-470.
- Batchelor, G. K. (2000). *An Introduction to Fluid Dynamics*. Cambridge: Cambridge University Press.
- Cleary, P. W. and J. J. Monaghan (1999). Conduction modelling using smoothed particle hydrodynamics. *Journal of Computational Physics* 148, 227-264.
- Dalrymple, R. A., O. Knio, D. T. Cox, M. Gesteira and S. Zou (2002). Using a Lagrangian particle method for deck over-topping. *Ocean Wave Measurement and Analysis* 1082-1091.
- Fick, A. (1855). Ueber diffusion. *Annalen der Physik* 170, 59-86.
- Fischer, H., E. List, R. Koh and J. Imberger, (1979). *Mixing in inland and coastal waters*. London: Academic.
- Gingold, R. A. and J. J. Monaghan (1977). Smoothed particle hydrodynamics: theory and application to non-spherical stars, Monthly notices of the royal astronomical society. *Monthly notices of the royal astronomical society* 181(3), 375-389.
- Grenier, N., M. Antuono, A. Colagrossi, D. L. Touz and B. Alessandrini (2009). An Hamiltonian interface SPH formulation for multi-fluid and free surface flows. *Journal of Computational Physics* 228(22), 8380-8393.
- Grenier, N., D. Le Touzé, A. Colagrossi, M. Antuono and G. Colicchio (2013). Viscous bubbly flow simulation with an interface SPH model. *Ocean Engineering* 69, 88-102.
- Hu, X. Y. and N. A. Adams (2006). A multi-phase SPH method for macroscopic and mesoscopic flows. *Journal of Computational Physics* 213(2), 844-861.
- Hua, J. and J. Lou (2007). Numerical simulation of bubble rising in viscous liquid. *Journal of Computational Physics* 222(2), 769-795.
- Lo, E. Y. and S. Shao (2002). Simulation of near-shore solitary wave mechanics by an incompressible SPH method. *Applied Ocean Research* 24(5), 275-286.
- Lucy, L. B. (1977). A numerical approach to the testing of the fission hypothesis. *The astronomical journal* 82, 1013-1024.
- Monaghan, J. and A. Kos (1999). Solitary waves on a Cretan beach. *Journal of waterway, port, coastal, and ocean engineering* 125, 145-155.
- Monaghan, J. and A. Rafiee (2013). A simple SPH algorithm for multi-fluid flow with high density ratios. *International Journal for Numerical Methods in Fluids* 71(5), 537-561.
- Monaghan, J. J. (1989). On the problem of penetration in particle methods. *Journal of Computational Physics* 82, 1-15.
- Monaghan, J. J. (1992). Smoothed Particle Hydrodynamics, Annual Review of Astronomy and Astrophysics. *Annual Review of Astronomy and Astrophysics* 30, 543-574.
- Monaghan, J. J. (1994). Simulating Free Surface Flows with SPH. *Journal of Computational Physics* 110(2), 399-406.
- Monaghan, J. J. (2005). Smoothed particle hydrodynamics. *Reports on progress in physics* 68(8), 1703.
- Monaghan, J. J. (2011). A turbulence model for smoothed particle hydrodynamics. *European Journal of Mechanics-B/Fluids* 30(4), 360-370.
- Morris, J. P. (2000). Simulating surface tension with smoothed particle hydrodynamics. *International Journal for Numerical Methods in Fluids* 33, 333-353.
- Morris, J. P., P. J. Fox and Y. Zhu (1997). Modeling Low Reynolds Number Incompressible Flows Using SPH. *Journal of Computational Physics* 136(1), 214-226.
- Omidvar, P. and P. Nikeghbali (2017). Simulation of violent water flows over a movable bed using smoothed particle hydrodynamics. *Journal of Marine Science and Technology* 22(2), 270-287.
- Omidvar, P., H. Norouzi and A. Zarghami (2015). Smoothed particle hydrodynamics for water wave propagation in a channel. *International Journal of Modern Physics C* 26(08), 1550085.

- Omidvar, P., P. K. Stansby and B. D. Rogers (2012). Wave body interaction in 2D using smoothed particle hydrodynamics (SPH) with variable particle mass. *International Journal for Numerical Methods in Fluids* 68(6), 686-705.
- Pourabdian, M., P. Omidvar and M. R. Morad (2017). Multiphase simulation of liquid jet breakup using smoothed particle hydrodynamics. *International Journal of Modern Physics C* 28(04), 1750054.
- Rostami, M. and P. Omidvar (2018). Smoothed-Particle- Hydrodynamics for the pattern of multi rising droplets. *Journal of Fluid Engineering* 140(8):081105.
- Shao, S. (2012). Incompressible smoothed particle hydrodynamics simulation of multifluid flows. *International Journal for Numerical Methods in Fluids* 69(11), 1715-1735.
- Shao, S. & Lo, E. Y. (2003). Incompressible SPH method for simulating Newtonian and non-Newtonian flows with a free surface. *Advances in water resources* 26(7), 787-800.
- Sultana, Z. (2012). *Finite Element Simulation of Interfacial Flows on Unstructured Meshes using a Second-Order Accurate VOF Method*. thesis, University of Toronto.
- Violeau, D. and B. D. Rogers (2016). Smoothed particle hydrodynamics (SPH) for free-surface flows: past, present and future. *Journal of Hydraulic Research* 54(1), 1-26.
- Wendland, H. (1995). Piecewise polynomial, positive definite and compactly supported radial functions of minimal degree. *Advances in computational Mathematics* 4(1), 389-396.
- Zheng, K., Z. C., Sun, J. W. Sun, Z. M. Zhang, G. P. Yang and Z. Feng (2009). Numerical simulations of water wave dynamics based on SPH methods. *Journal of Hydrodynamics, Ser. B* 21(6), 843-850.